Diffractive optical elements with square concentric rings of equal width

Javier Alda[1], Luis Miguel Sanchez-Brea[2], Francisco Javier Salgado-Remacha[2], and José María Rico-García[2,3]

Applied Optics Complutense Group,

Optics Department, University Complutense of Madrid,

[1] School of Optics. Ave. Arcos del Jalón, 118, 28037 Madrid, Spain

[2] Physics Faculty, Av Complutense, s/n, 28040

[3]Rico-Garcia is currently with Centre de Recherche Paul Pascal, Bourdeax, France

Corresponding author: Javier Alda

Phone: +34 91 394 68 74, Fax: +34 91 394 68 85

E-mail: j.alda@opt.ucm.es

Abstract

A diffractive optical element having equal-width concentric square rings is analyzed in this paper. This constant width makes possible its realization using spatial light modulators or square pixels phase screens. It allows a simple analytical treatment. The element is also simulated using the Rayleigh-Sommerfeld approach. An experimental verification of its performance has been compared with the simulated results.

Keywords: diffractive optics. Fresnel zone plates.

1 Introduction

A Fresnel zone plate is a diffractive element able to be integrated in micro-optical devices. Its performance is based on the interference of successive zones typically arranged following a phase-shift pattern, being the Fresnel zones the simplest solution. [1]. The typical design for a Fresnel Zone Plate (FZP) has circular shape zones and circular symmetry, like a refractive lens. Although, it can be adapted to some other conformal geometries and off-axis operation [2]. These zones are also know as semi-periodic zones because the phase of the total amplitude arriving to the image point from the location of a given zone is shifted in π with respect to the phase coming from the adjacent zones. An alternative to a Circular Zone Plate is a Polygonal Fresnel Zone Plate (PFZP) [3]. When the number of sides of the polygon is low, the balance between the high-focusing performance of a circular zone plate and the easiness of fabrication at micro and nano-scales of polygons represents a high advantage for the polygonal designs. The simplest polygonal shape is a triangle, although the square, due to its natural fitting to the rectangular coordinate system, has deserved special attention [3], [4]. The design of a Square Fresnel Zone Plates (SFZP) optimizes it to perform as close as possible as a circular Fresnel Zone Plate. In a previous work [5], we have studied a SFZP design based on the minimization of the difference between the area covered by the angular sector of the zone of the corresponding circular plate and the one covered by the polygon traced on the plate. In the present contribution we propose an alternative design for SFZP. In this case, the distance between the borders of consecutive zones is constant along the SFZP. We propose this design because of the practical realization that we made of those SFZP using Spatial Light Modulators having square pixels in a

square arrangement. The border between consecutive zones of our previous designs we falling at a given pixel that shared phase differences belonging to two consecutive zones. When going farther from the center of the SFZP, this situation becomes more prevalent and the devices fails to perform as expected. Then, we have avoided the existence of shared pixels by setting a constant width for each SFZP. In this case the border between zones coincides with the border of the pixel. We think that this design is more appropriate for its realization using Spatial Light Modulator, or pixelated phase screens. There are several situations where this approach can be useful. For example, in the development of IR reflectarrays where phase shift is depending on the resonance of subwavelength elements coupled along a given area [6].

Section 2 of this paper introduces the analytical solution to build a phase mask having concentric rings with a constant width, and a constant phase within each ring. Section 3 shows the results obtained from the simulation using the Rayleigh-Sommerfeld approach [7] and from the experiment made with a Spatial Light Modulator (SLM). Finally, section 4 summarizes the main conclusions found in this study.

2 Theory

The analysis of the square Fresnel zones can be derived from the evaluation of the amplitude distribution obtained along the optical axis for a square aperture. This optical axis is perpendicular to the plane of the diffractive element and crosses the center of the square aperture.

Following Goodman [8] we may find that the amplitude obtained at a distance z after a square aperture having an apothem value of a, is given as,

$$E(x,y)=\frac{e^{ikz}}{i\lambda z}\int_{-a}^{a}\int_{-a}^{a}\exp\left\{i\frac{\pi}{\lambda z}\left[\left(x-\xi\right)^2+\left(y-\eta\right)^2\right]\right\}d\xi d\eta\,, \tag{1}$$

where (ξ,η) are the coordinates within the plane of the aperture, (x,y) are the coordinates at the plane of interest, and λ is the wavelength. When applied to a focusing diffractive element the observation plane is placed at the focal distance from the lens, $z=f$, and the location of interest is at $(x=0,y=0)$, where the light beam is focused. Due to the symmetry of the problem, this equation can be factorized in two one-dimensional integrals.

$$E(0,0)=\frac{e^{ikz}}{i}I^2(a), \tag{2}$$

where

$$I(a)=\frac{1}{\sqrt{\lambda z}}\int_{-a}^{a}\exp\left(i\frac{\pi}{\lambda z}u^2\right)du, \tag{3}$$

u is a dummy integration variable, and a is the apothem of the square aperture. Using the following change of variables, $\alpha=u\sqrt{2/(\lambda z)}$, the function $I(a)$ can be written as

$$I(a)=\sqrt{2}\left[C\left(\sqrt{2\frac{a^2}{\lambda f}}\right)+iS\left(\sqrt{2\frac{a^2}{\lambda f}}\right)\right], \tag{4}$$

where C and S represent the Fresnel integrals. Substituting this function in Eq. (2) for the electric field at the focal point, we find the amplitude at the focal point as:

$$E(0,0)=-2ie^{ikz}\left[C\left(\sqrt{2\frac{a^2}{\lambda f}}\right)+iS\left(\sqrt{2\frac{a^2}{\lambda f}}\right)\right]^2. \tag{5}$$

This complex amplitude has been represented in figure 1 as the thick solid spiral curve. As far as we are interested in the contribution of a given concentric square polygon, we may calculate this contribution as

$$E_{ring}(x,y)=E_{outer}(x,y)-E_{inner}(x,y), \tag{6}$$

being E_{outer}, and E_{inner} the amplitudes corresponding to the square apertures limiting the ring. The general expression of this amplitude was given by Eq. (5). Therefore, the analytical expression for the amplitude of the ring is

$$E_{ring}(x,y) = -2i\exp(ikz)\left[\left(C_{outer}+iS_{outer}\right)^2-\left(C_{inner}+iS_{inner}\right)^2\right], \tag{7}$$

where C_{outer}, S_{outer}, C_{inner} and S_{inner} represent the Fresnel integrals calculated for the inner and outer limits of the square ring. The complex representation of these amplitudes has been plotted in figure 1 as think solid lines joining those points representing the location of the inner and outer borders of the zone The phase associated to this amplitude can be written as

$$\text{Phase}\left[E_{ring}\right] = \tan^{-1}\left[kz + \frac{2\left(C_{outer}S_{outer}-C_{inner}S_{inner}\right)}{\left(C_{outer}^2-C_{inner}^2\right)-\left(S_{outer}^2-S_{inner}^2\right)}\right]. \tag{8}$$

The phase of the amplitude of each zone is represented as the angle of the complex amplitude plotted in figure 1. The amplitude of each zone can be calculated as the amplitude vector departing from the location of the apothem of the inner square and reaching the location of the apothem of the outer square in the amplitude curve. A way of optimizing the focusing of a diffractive element built with concentric square ring is to compensate continuously the phase of each ring in order to add the corresponding amplitude in phase. In the limit of an infinitesimal width square ring the resulting amplitude can be seen as the length of the complex amplitude curve represented in 1.

In a previous contribution [5], we have experimentally analyzed the case of an optimized Fresnel zoning having zones with a prescribed apothem. In this case we are mostly interested in a different zoning strategy. Our case here is not following the Fresnel zoning strategy, but is dealing with square rings having the same width. Then,

the apothems of the inner and outer squares limiting the ring can be written as $a_m = m\Delta a$, where Δa is the constant width of the rings. As we mentioned above, by reducing this width we may increase the total amplitude of the square FZP. This can be seen in Figure 1 where two different widths have been compared for a better understanding of the influence of the width of the zone. However, in practice this width is finite and some limitation in the performance of the diffractive element should happen. The limit appears when the width is comparable with the width of the Fresnel zone. As far as the Fresnel zones are decreasing their widths when moving outward the center of the lens, this limitation will appear for a given aperture. We may write this condition as

$$\Delta a = \sqrt{\lambda f\,(m+1)} - \sqrt{\lambda f\, m}\,. \tag{9}$$

If we assume that the number of Fresnel zones covered by the diffractive element, m, is large enough, we may apply some approximation and establish a limiting value for m, that is $m \simeq \lambda f \big/ (\Delta a)^2$, corresponding to an apothem value of

$$a_{\lim} \simeq \frac{\lambda f}{\Delta a}\,. \tag{10}$$

We can use the developed expressions in order to obtain an analytical solution for the irradiance distribution around the focus of this SFZP. However, for the good of simplicity and clarity of the analysis, we preferred to perform a numerical analysis to determine the focusing capabilities of this lens. For the numerical implementation, we have used a fast-Fourier-transform based direct-integration method which uses the Rayleigh-Sommerfeld approach [7]. This scalar approach is valid as long as the features of the SFZP are larger than the wavelength. In addition, the proposed algorithm presents

a quality parameter which indicates when the simulation is done properly. In Section 3 we will see a comparison between numerical analysis and experimental approach.

3 Experimental Results

A map of the phase introduced in our Spatial Light Modulator is given in figure 2 as a gray level image. The experimental set-up is described in Fig. 3. We use a Spatial Light Modulator (SLM) to simulate a collection of SFZP described in previous section. The SLM is a Holoeye LCR-2500 reflective modulator, with 1024x768 pixels (8 bits resolution), driven by the graphic board of a PC. A He-Ne laser ($\lambda = 632.8\,nm$) is employed as a coherent light source. Two linear polarizers (P1 and P2) are used to control the intensity of the laser. A Spatial Filter (SF) is needed, in order to obtain a pure-gaussian collimated beam. The Spatial Filter consists of a $40\times$ microscope objective, conjugated with a $10\,\mu m$ pinhole. Setting the pinhole in the focal point of the microscope objective, we ensure a Gaussian-like beam illumination onto the SLM. Then, a Collimation Lens (CL) is chosen to collimate the beam with the proper size to illuminate completely the lens mask over SLM. A 50/50 Beam-Splitter (BS) is placed at 45º with the propagation axis, so we can illuminate the SLM normally to its surface. At the same time, a BS guides the modulated light to a UI-1220-M camera from U-Eye (CMOS), with a pixel pitch of $6\,\mu m$. CMOS is free to travel along the beam propagation axis, so we can make any measurements at any desired plane. SLM adds a considerable amount of aberrations to the wavefront of the reflected beam due to the fabrication process. Therefore, the phase of a suitable astigmatic lens is added to the phase map of the Fresnel lens to eliminate the astigmatism. The phase of this elliptical correction lens is

$$\phi_{elliptical} = \frac{\pi}{\lambda}\left[\left(\frac{x\cos\theta + y\sin\theta}{\sqrt{f_1}}\right)^2 + \left(\frac{-x\sin\theta + y\cos\theta}{\sqrt{f_2}}\right)^2\right] \tag{11}$$

where the parameters f_1 and f_2 are the Sturm foci and θ is the angle between the lens axes and the laboratory axes. These parameters are experimentally adjusted until no aberrations are observed resulting $f_1 = 14$ m, $f_2 = 8$ m, and $\theta = -167.7^\circ$.

In order to adapt the square Fresnel zones geometry, as much as possible to the SLM, we have designed them taking into consideration the pixel size and period, which is 19 μm along a square grid. Consequently, the pixels are oriented in the regular grid with this period for the directions *x* and *y*.

We have measured the power at focus for a set of lenses varying Δa from one lens to another. At the same time, the Rayleigh-Sommerfeld integral approach has been employed to get the corresponding theoretical curve. Moreover, a linear fit has been achieved when the number of zones is low. The values for the linear regression are $I = I_0 + \alpha m$ where m is the number of zones, $I_0 = -0.10 \pm 0.01$ and $\alpha = 0.0312 \pm 0.0003$. The linear regression coefficient is $R = 0.94$ (Fig. 4). The conditions for the simulations are similar to those of the experimental set-up we have explained. We have to take into account, for example, the wavelength of the laser λ, and the pixel size of the SFZP, 19 μm. For the simulations we have performed a re-sampling of the SFZP so that the pixel size in the propagation algorithm is similar to the pixel size of the camera (6 μm).

The results, along with the predictions from the simulation are shown in Fig. 4 for SFZP with equal width between zones. We show the results in irradiance at the focus as a

function of the apothem for different values of Δa. For the experimental measurement, a collection of lenses has been projected onto the SLM, characterized all them by the same focal distance, $f' = 0.5m$ but with different Δa. For each lens, a map of the intensity has been recorded at the focal plane. Five images were acquired and averaged for each map to minimize noise. These averaged images are used in the analysis in order to obtain the intensity at the focus. The gain of the camera has been adjusted at a level that keeps the pixel under saturation for the complete set of lenses.

We may see that when the width of the zone is narrower, the irradiance is closer to the continuous case solution and stabilizes its growing for an apothem value closely located around the value given by the previous Eq. (10). When increasing the number of zones further, the irradiance at focus increases at a slower rate in comparison to lenses with a low number of zones.

In addition, different images of the intensity at focus for each kind of lens have been acquired with the camera. In Fig. 5 the Rayleigh-Sommerfeld predictions are displayed. Fig. 6 depicts the experimental results for the phase distributions projected on the SLM for Fig. 5. Both figures show the spatial intensity pattern in pre-focal, focal and post-focal planes. As it can be noticed out from the collected data, theory and experiments fit well with the experimental results.

Another point to be remarked is the symmetry of the intensity spatial distribution for different SFZPs. Despite the fact there is no symmetry between the post-focal and the pre-focal plane for the customized SFZP family [5], this is not the case for an equal-width SFZP.

4 Conclusions

A new design of Square Zones Plates diffractive elements is described in this work. The main attribute of this design is the equal-width restriction of the zones. Although its optical behavior is quite enough to act as diffractive focusing element, its efficiency is not as good as a Circular Fresnel Lens. Nevertheless, the easiness to manufacture them suggests a deep analysis of its optical characteristics. Besides, the square symmetry allows for an easy analytical treatment. The irradiance at the focus increases linearly with the number of zones included in the design. The behavior of these lenses has been numerically proven using a numerical implementation of the Rayleigh-Sommerfeld approach. In addition, an experimental verification has been performed using a Spatial Light Modulator for implementing the designed Square Fresnel Zones Plates. The agreement between the experimental measurements and the numerical simulations proves the feasibility of these diffractive optical elements for micro and nano-optics applications.

Acknowledgments

This work has been partially supported by project TEC2006-1882 of the Ministerio de Educación of Spain, and project CCG08-UCM/DPI-3952 of "Dirección General de Universidades e Investigación de la Consejería de Educación de la Comunidad de Madrid" y "Universidad Complutense de Madrid". Salgado-Remacha acknowledges the economical support of "Ministerio de Educación y Ciencia" and the European Social Fund.

References

[1] E. Hecht, “Optics”, Addisson Wesley, Reading, Mass, USA 2001.

[2] H. D. Hristov, “Fresnel zones in wireless links, zone plate lenses and antennas”, Artech House, Norwood, MA, USA, 2000.

[3] J. Alda, G. Boreman, “Optimization of polygonal Fresnel zone plates” Microwave Opt. Technol. Lett. 50 (2008) 536-541.

[4] I. V. Minin, O. V. Minin, A. Petosa, S. Thirakuone, Microwave Opt. Technol. Lett., “Improved zoning rule for designing square fresnel zone plate lenses” 49 (2007) 276-278.

[5] Javier J. Alda, J.M. Rico-García, F.J. Salgado-Remacha, L.M. Sanchez-Brea. Opt. Comm. “Diffractive performance of square Fresnel zone plates”, In press (2009) doi:10.1016/j.optcom.2009.05.05

[6] J. Ginn, B. Lail, J. Alda, G. Boreman, “Planar infrared binary phase reflectarray” Opt. Lett. 33 (2008) 779-781.

[7] F. Shen and A. Wang, “Fast-Fourier-transform based numerical integration method for the Rayleigh-Sommerfield diffraction formula” Appl. Opt. 45 (2006) 1102-1110.

[8] J. W. Goodman, “Introduction to Fourier Optics”, 3rd edition. Roberts & Company, Englewood, Colorado, USA, 2005.

Figure captions

Fig. 1. Representation of the complex amplitude for two different values of the width of the square zones. The dots represent the location of the equal width borders. The lines joining those dots represent the complex amplitude of the zone. Its length is the modulus and the angle in the complex plane represent the phase. When the width is narrower the amplitude of the successive zones approaches better to the exact amplitude curve. The values of the parameters used in this analysis are: λ= 633 nm, and f =50 cm. The width of the square concentric rings is 19 μm for the top plot and 95 μm for the bottom plot.

Fig. 2. 20 zone equal width SFZP with customized periodic pattern of phases according to the computation method mentioned.

Fig. 3. Experimetnal Set-Up. He-Ne: Light source, He-Ne laser ($\lambda = 632.8\,nm$). P1 and P2: two linear polarizers. SF: the Spatial Filter. CL: Collimation Lens (CL). BS: 50/50 Beam-Splitter. CMOS: UI-1220-M camera from U-Eye. CMOS is free to travel along the beam propagation axis.

Fig. 4. Experimental (dots), computation (continuous line) and linear fit (dashed line) to the dependence of the irradiance at focus as a function of the apothem for different values of Δa. The irradiance has been normalized to its maximum.

Fig. 5. Computed equal-width SFZP intensity patterns (f=0.5, Number of Zones: 30, wavelength $\lambda = 633\,\mathrm{nm}$). From left to right: Prefocal, focal and post-focal planes of observation, $z = f - 1cm$, $z = f$ and $z = f + 1cm$ respectively.

Fig. 6 Measured equal-width SFZP intensity patterns. (f=0.5, Number of Zones: 60, wavelength $\lambda = 633\,\mathrm{nm}$). From left to right: Prefocal, focal and post-focal planes of observation, $z = f - 1cm$, $z = f$ and $z = f + 1cm$ respectively..

FIGURE 1

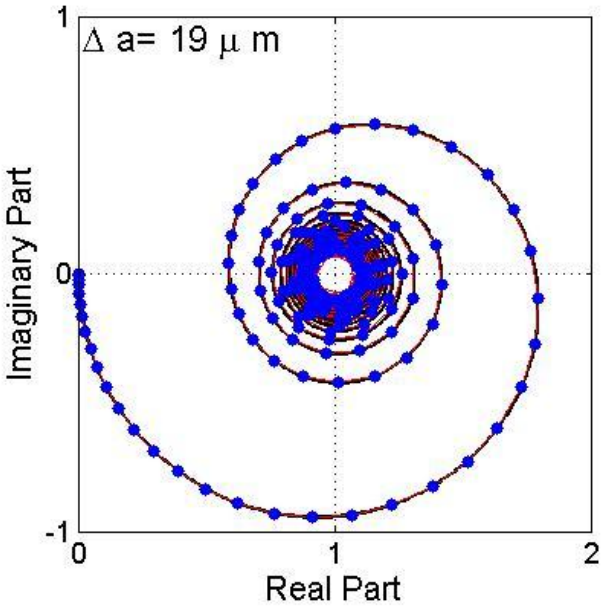
Δ a= 19 μ m
Imaginary Part
Real Part
1
0
-1
0
1
2

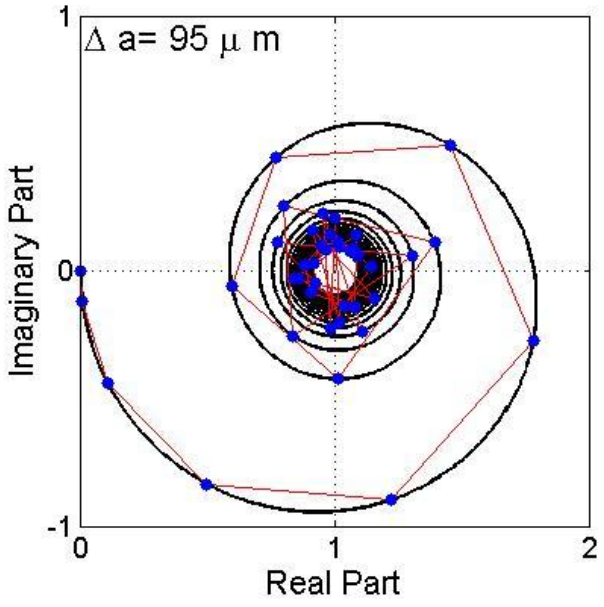
Δ a= 95 μ m
Imaginary Part
Real Part
1
0
-1
0
1
2

FIGURE 2

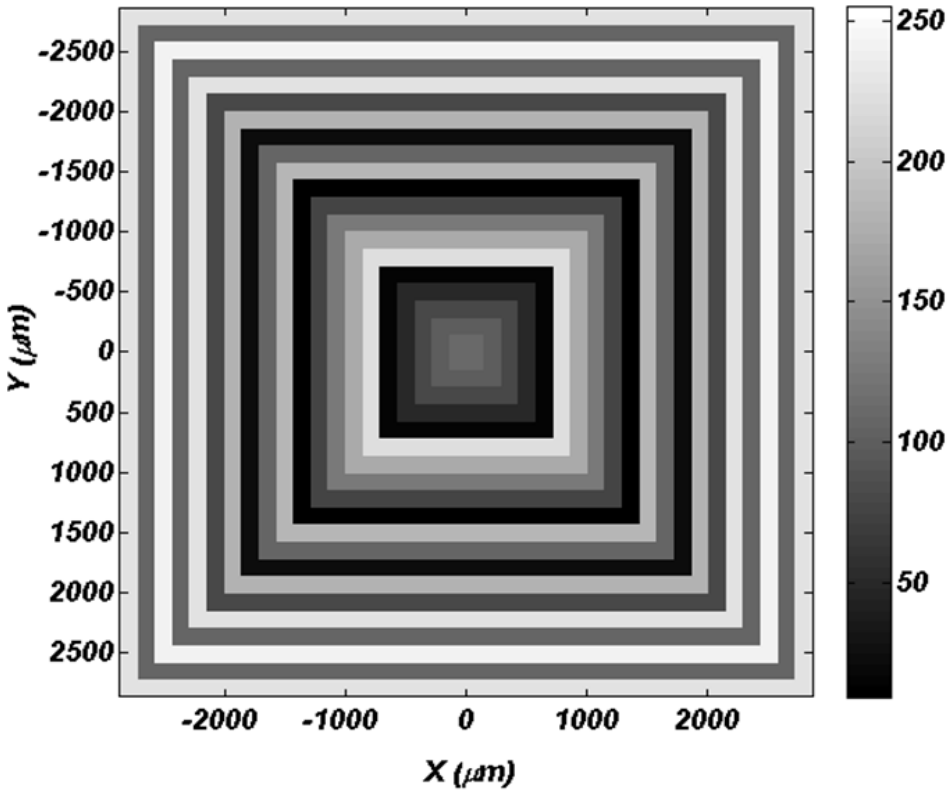
-2500
-2000
-1500
-1000
-500
0
500
1000
1500
2000
2500
Y (μm)
-2000
-1000
0
1000
2000
X (μm)
250
200
150
100
50

FIGURE 3

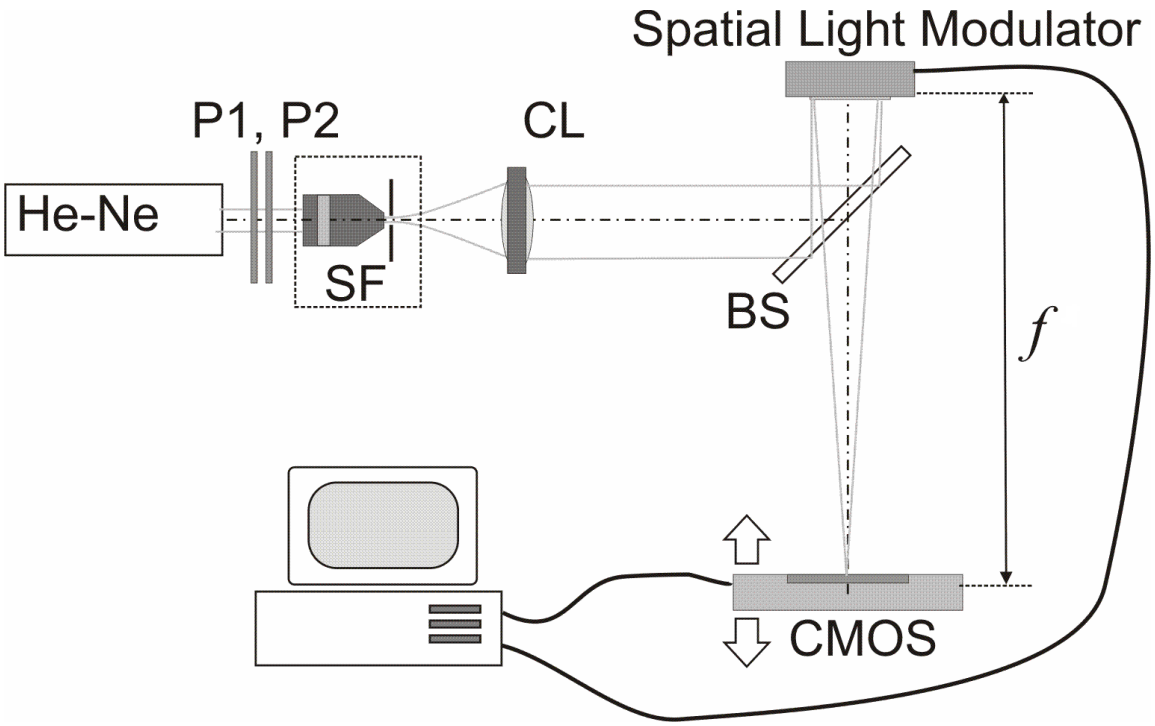

FIGURE 4

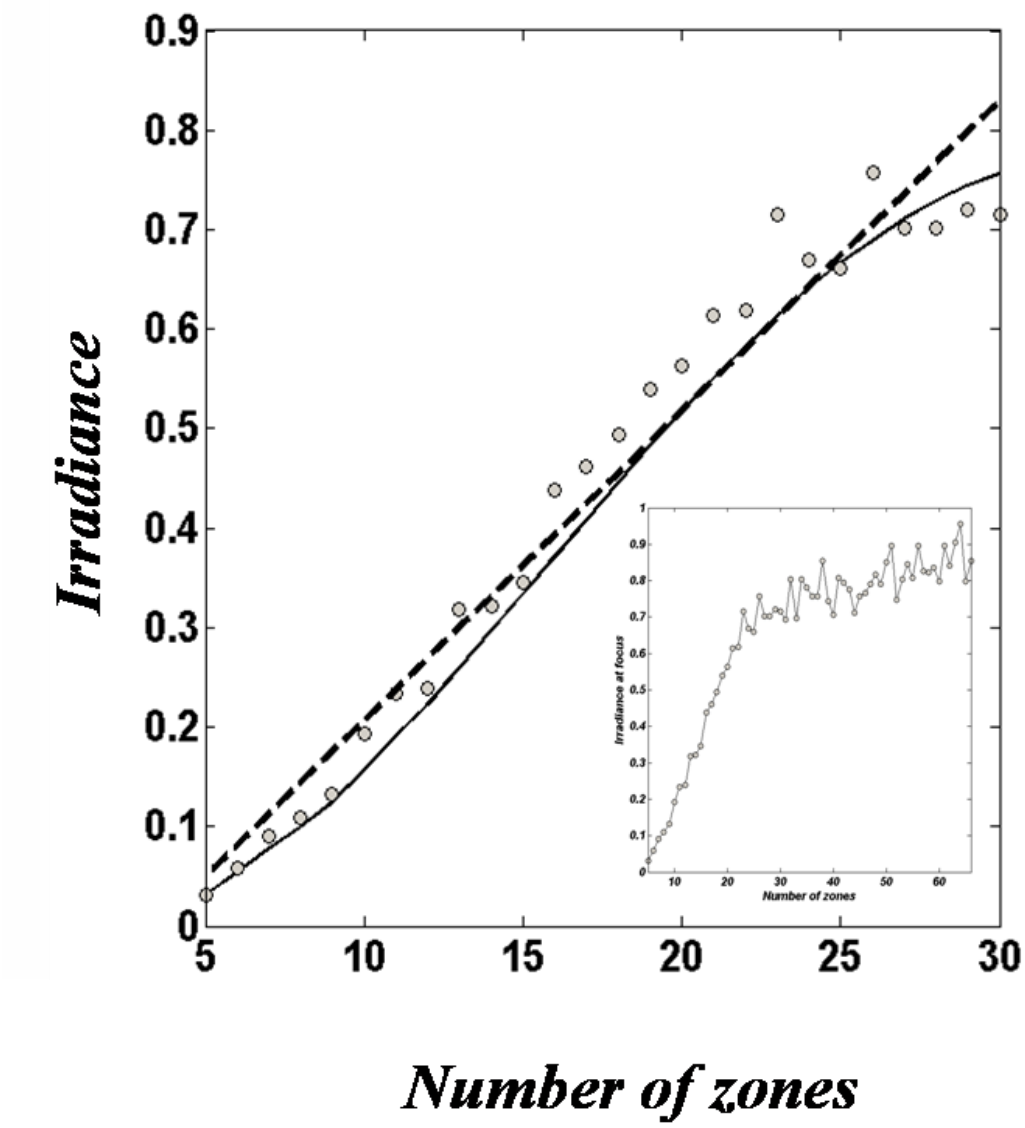
Irradiance
0.9
0.8
0.7
0.6
0.5
0.4
0.3
0.2
0.1
0
5
10
15
20
25
30
Irradiance at focus
Number of zones
Number of zones

FIGURE 5

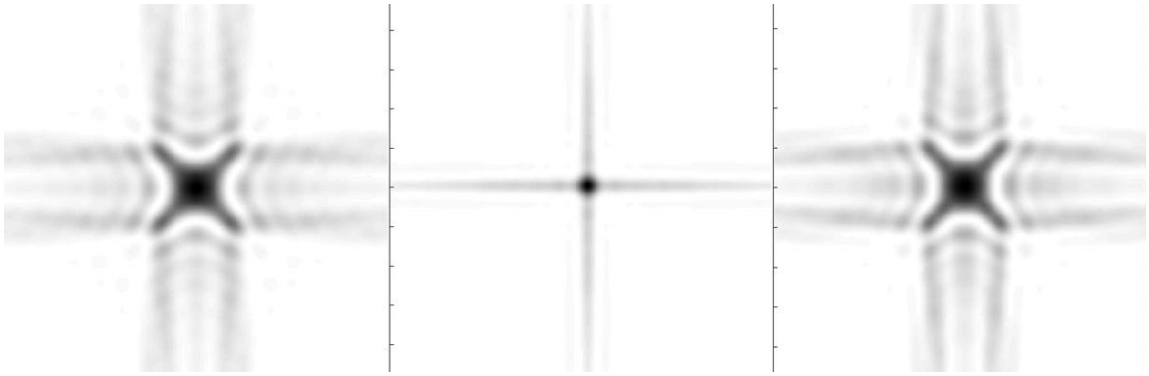

FIGURE 6